Received: 17 December 2019 | Revised: 9 May 2020 | Accepted: 19 May 2020

DOI: 10.1111/all.14451

ORIGINAL ARTICLE

Atopic Dermatitis, Urticaria and Skin Disease

Allergy EUROPEAN JOURNAL OF ALLERGY AND CLINICAL IMMUNOLOGY EAACI WILEY

Inhibition of mite-induced dermatitis, pruritus, and nerve sprouting in mice by the endothelin receptor antagonist bosentan

Makiko Kido-Nakahara[1] | Bing Wang[1] | Fumitaka Ohno[1] | Gaku Tsuji[1,2] | Dugarmaa Ulzii[1,3] | Masaki Takemura[1] | Masutaka Furue[1,2,4] | Takeshi Nakahara[1,4]

[1]Department of Dermatology, Graduate School of Medical Sciences, Kyushu University, Fukuoka, Japan

[2]Research and Clinical Center for Yusho and Dioxin, Kyushu University Hospital, Fukuoka, Japan

[3]Department of Dermatology, National Dermatology Center of Mongolia, Ulaanbaatar, Mongolia

[4]Division of Skin Surface Sensing, Graduate School of Medical Sciences, Kyushu University, Fukuoka, Japan

Correspondence
Makiko Kido-Nakahara, Department of Dermatology, Graduate School of Medical Sciences, Kyushu University, 3-1-1 Maidashi, Higashi-ku, Fukuoka 812-8582, Japan.
Email: macky@dermatol.med.kyushu-u.ac.jp

Abstract

Background: Endothelin-1 (EDN1) can evoke histamine-independent pruritus in mammals and is upregulated in the lesional epidermis of atopic dermatitis (AD). EDN1 increases the production of interleukin 25 (IL-25) from keratinocytes to accelerate T helper type 2 immune deviation. Plasma EDN1 levels are positively correlated with the clinical severity and itch intensity of AD. Therefore, we hypothesized that the inhibition of EDN1 might be useful for treating atopic inflammation and itch and investigated the effects of the topical application of the EDN1 receptor antagonist bosentan on the skin inflammation and itch in a murine AD model.

Methods: We analyzed the mite-induced AD-like NC/Nga murine model, which was topically applied with bosentan or ethanol control every day for 3 weeks. We also subjected in vitro primary sensory neuron culture systems to nerve elongation and branching assays after EDN1 stimulation.

Results: Topical application of bosentan significantly attenuated the development of mite-induced AD-like skin inflammation, dermatitis scores, ear thickness, scratching bouts, and serum level of thymus and activation-regulated chemokine in NC/Nga mice. Bosentan application also significantly reduced the gene expression of *Il13*, *Il17*, and *Ifng* in the treated lesions. Histologically, the number of infiltrated dermal cells, the epidermal EDN1 expression, and the number of intraepidermal nerve fibers were significantly inhibited upon bosentan application. While EDN1 significantly elongated the neurites of dorsal root ganglion cells in a dose- and time-dependent manner, bosentan treatment attenuated this.

Conclusions: EDN1 plays a significant role in mite-induced inflammation and itch. Topical bosentan is a potential protective candidate for AD.

KEYWORDS

atopic dermatitis, endothelin receptor, endothelin-1, nerve elongation, pruritus

Abbreviations: AD, atopic dermatitis; DRG, dorsal root ganglion; EDN1, endothelin 1; EDNR, endothelin receptor; ERK, extracellular signal-regulated kinase; IL, interleukin; ILC2, group 2 innate lymphoid cell; JNK, c-Jun N-terminal kinase; MAPK, mitogen-activated protein kinase; MEK, mitogen-activated protein kinase kinase; NHEK, normal human epidermal keratinocyte; PGP9.5, protein gene product 9.5; qRT-PCR, quantitative real-time polymerase chain reaction; SDS, sodium dodecyl sulfate; TARC, thymus and activation-regulated chemokine; Th2 cell, T helper 2 cell.

© 2020 EAACI and John Wiley and Sons A/S. Published by John Wiley and Sons Ltd.

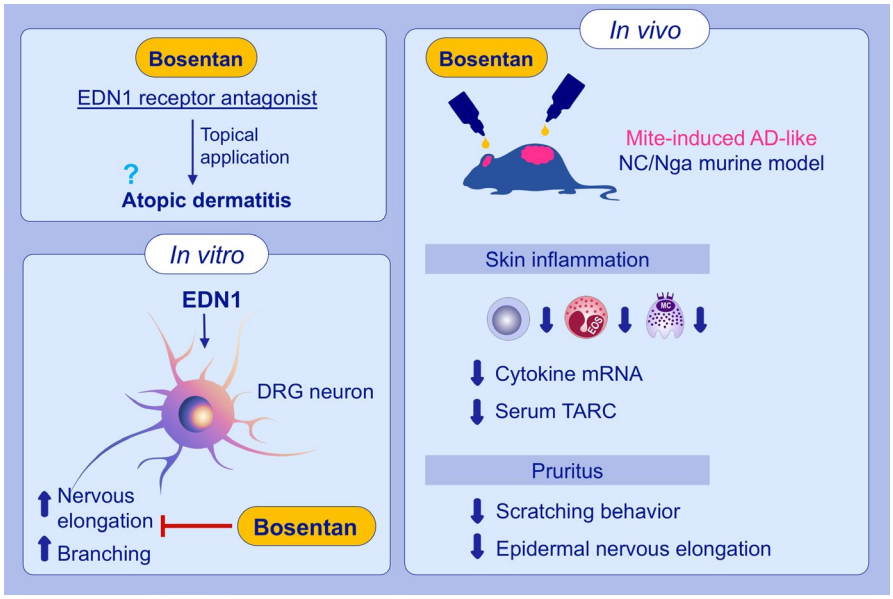

GRAPHICAL ABSTRACT

Topical application of EDN1 receptor antagonist, bosentan, significantly attenuated the development of mite induced AD-like skin inflammation, scratching bouts and epidermal nervous elongation in NC/Nga mice. While EDN1 significantly elongated the nerves of dorsal root ganglion cells, bosentan treatment attenuated this. Topical bosentan is a potential protective candidate for AD.

1 | INTRODUCTION

Atopic dermatitis (AD) is a common, chronic, severely pruritic, eczematous skin disease, which markedly deteriorates the quality of life of those afflicted by it.[1,2] Besides intense itch, AD is characterized by skin inflammation and barrier dysfunctions.[1,3] Severe and chronic pruritus induces inevitable scratching and the vicious itch/scratch cycle exacerbates and sustains the atopic inflammation and skin barrier dysfunction.[4] The acute skin lesions of AD exhibit a T helper type 2 (Th2)-deviated reaction, but at the chronic stage, Th1- and Th17-related cytokines and chemokines also intermingle and perpetuate the skin inflammation. The skin microbiome and the autoallergic inflammation are also related to the pathological condition of AD.[5,6] Moreover, many peptides and proteases have been shown to play important roles in the pathophysiology of AD.[2,7]

Endothelin-1 (EDN1) is a 21-amino-acid peptide that is expressed by a variety of cell types, including endothelial cells, immune cells such as dendritic cells, monocytes, and macrophages, neurons, and keratinocytes.[8-13] In addition to its potent vasoconstricting activity, EDN1 is also involved in keratinocyte proliferation, neo-angiogenesis, and leukocyte chemotaxis.[14-16] Increased EDN1 expression is closely associated with pathogenetic mechanisms of several diseases such as scleroderma and asthma.[17,18] EDN1 also acts as a potent pruritogen in mice[19,20] and humans,[21] and induces itch by directly activating sensory neurons.[22] Moreover, plasma EDN1 levels have been shown to be elevated and positively correlated with clinical severity, itch intensity, and serum IgE level in AD.[23] We also demonstrated that EDN1 amplified epidermal inflammation via mutual positive feedback between EDN1 and IL-25,[24] which is one of the main activators of group 2 innate lymphoid cells (ILC2),[25] and that EDN1 polarized the dendritic-cell-T-cell response toward Th17/1 differentiation.[26] Therefore, EDN1 could be suggested to induce the promotion of both type 1/17 inflammation (at the immune synapsis level) and type 2 inflammation (via ILC2). Thus, we hypothesize that EDN1 may accelerate the chronicity of AD lesions. However, its role in atopic inflammation remains elusive.

EDN1 works via G-protein-coupled EDN receptor (EDNR) types A and B.[27] The binding of EDN1 to EDNR types A and B activates various signaling pathways including adenylyl cyclase signaling, phosphoinositide signaling, oxidative stress, growth factor receptor transactivation, and the mitogen-activated protein kinase (MAPK) pathway.[28] Bosentan is known as a potent antagonist that inhibits EDNR of both types A and B.[29] Bosentan tablets are used to treat pulmonary arterial hypertension in the United States, the European Union, Japan, and other countries. In addition to vasodilation, bosentan has been reported to have anti-inflammatory effects.[30,31] In this study, we examined the effects of bosentan on mite-antigen–induced AD-like model mice. We found that topical bosentan significantly reduced the clinical and histological inflammatory response as well as *Il13*, *Il17a*, and *Ifng* expression in AD mice. Bosentan also inhibited the itching/scratching behavior, the epidermal EDN1 expression, and the number of intraepidermal nerve fibers. Notably, EDN1 appeared to accelerate neurite elongation and branch formation of dorsal root ganglion (DRG) cells, which was inhibited by bosentan.

2 | METHODS

For several sections, additional details are provided in Data S1.

2.1 | Mice

Female NC/Nga mice aged 9-11 weeks old were used for the experiments on an AD-like murine model. Female C57BL/6 mice aged 6 weeks old were used for the experiment of DRG neuron elongation in vitro. The maintenance and experimental procedures of the mice were approved by the Animal Care and Use Committee of Kyushu University School of Medicine.

2.2 | Induction of mite-induced AD-like murine model

It is known that repeated epicutaneous application of mite-antigen induces AD-like dermatitis in NC/Nga mice.[32] In this study, the hair on their upper back was shaved with a clipper and removed with depilatory. The shaved dorsal back and ear skin was treated with 200 mL of 4% sodium dodecyl sulfate (SDS). These mice were topically treated with 200 mL of 5% bosentan (AD-bosentan group, n = 7) or vehicle (AD-ethanol group, n = 7; and control-ethanol group, n = 7) every day for 3 weeks on the same dorsal back and ear skin. After 1 or 2 hours, 100 mg of mite-antigen (*Dermatophagoides farinae* extract; Biostir AD) was epicutaneously applied to the same site where SDS and bosentan had been applied, twice a week for 3 weeks (AD-ethanol group and AD-bosentan group). On day 22, these mice were killed (Figure 1A).

2.3 | Evaluation of skin lesions

The clinical severity of dermatitis was evaluated at every timepoint of mite-antigen application. The development of (a) erythema/hemorrhage, (b) scaling/dryness, (c) edema, and (d) excoriation/erosion was scored as 0 (none), 1 (mild), 2 (moderate), or 3 (severe). The sum of the individual scores was taken as the dermatitis score.

2.4 | Evaluation of scratching behavior

Scratching behavior of the mice was measured for 4 hours immediately after the last stimulation of mite-antigen using the Microact1 system.

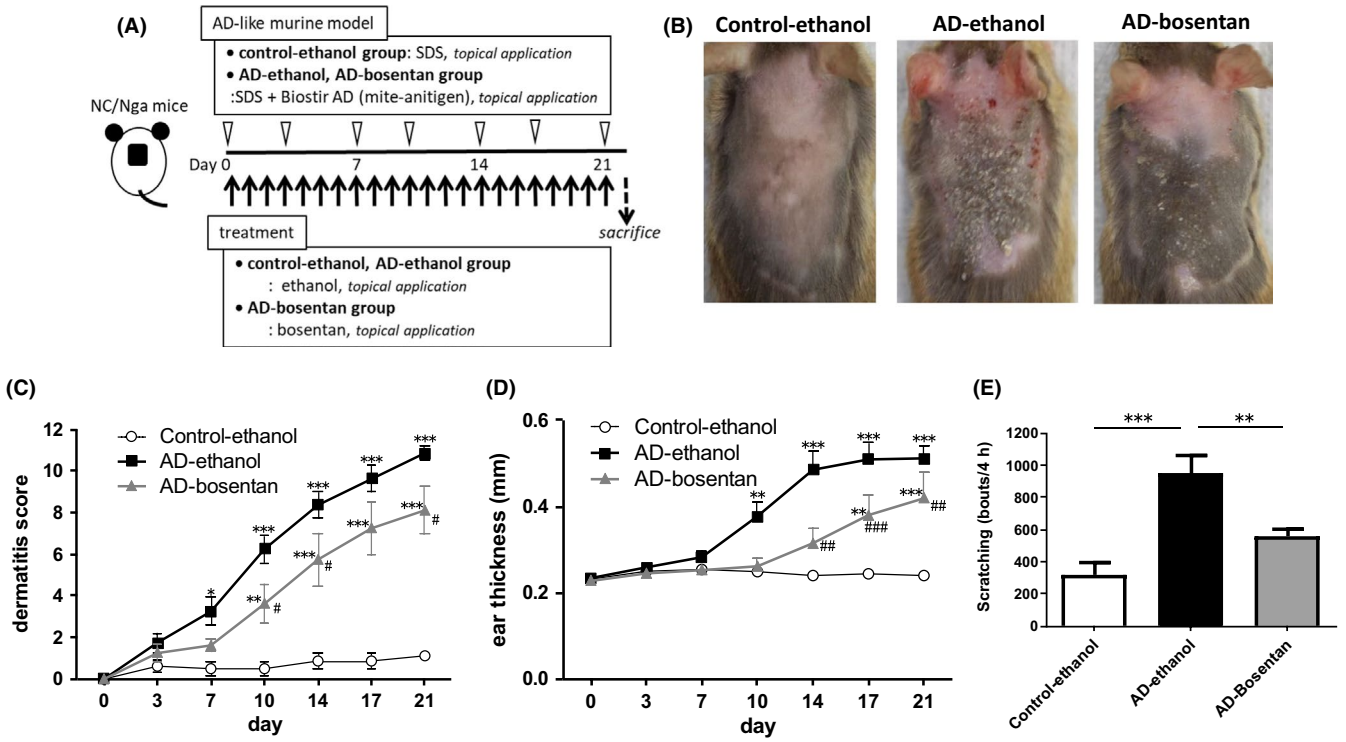

FIGURE 1 Bosentan provided relief of the mite-induced dermatitis symptoms in NC/Nga mice. (A) Schema of the animal model. These mice were topically treated with 200 mL of 5% bosentan (AD-bosentan group) or vehicle (AD-ethanol group and control-ethanol group) every day for 3 wk on the dorsal back and ear skin. After 1 or 2 h, 100 mg of mite-antigen (*Dermatophagoides farinae* extract; Biostir AD) was epicutaneously applied to the same site twice a week for 3 wk (AD-ethanol group and AD-bosentan group). (B) Macroscopic features of skin lesions of control-ethanol, AD-ethanol, and AD-bosentan groups on day 21. (C) Dermatitis scores were assessed at each time of mite-antigen stimulation. (D) Ear thickness was measured at each time of mite-antigen stimulation. (E) Scratching behavior was measured after the last mite-antigen stimulation for 4 h. (C, D) $^{*}P < .05$, $^{**}P < .01$, $^{***}P < .001$ compared with the control group. #$P < .05$, ##$P < .01$, ###$P < .001$ compared with the AD group. (E) $^{**}P < .01$, $^{***}P < .001$. Each group consisted of seven mice. Representative data of three independent experiments are shown

2.5 | ELISA

Serum obtained from the whole blood of NC/Nga mice was kept at − 80°C until further use. Quantikine ELISA Kit, eotaxin mouse SimpleStep ELISA Kit, and mouse Anti-HDM IgG Antibody Assay Kit were used for determining thymus and activation-regulated chemokine (TARC), eotaxin, and house dust mite IgG concentrations, respectively, in mouse serum, in accordance with the manufacturer's protocol.

2.6 | Primary DRG neuron culture

DRGs of C57BL/6 mice were dissociated from the lumbar, thoracic, and cervical regions after removing blood, and then treated with papain-cysteine solution containing 0.67 mg/mL L-cysteine, 2 mg/mL papain, and 0.2% (v/v) saturated $NaHCO_3$ in HBSS without Ca^{2+} or Mg^{2+}, and collagenase solution containing 3 mg/mL collagenase in HBSS without Ca^{2+} or Mg^{2+}, for 10 minutes each at 37°C. DRGs were triturated for dissociation to prepare a single-cell suspension in plating medium containing 10% FBS, 10% horse serum, 1.5 mg/mL glucose, 1% penicillin/streptomycin/glutamine, 2% B27, 140 μg/mL DNase, and 2 mmol/L GlutaMax in DMEM, followed by straining through a 70 μm cell strainer. DRG neurons were plated on poly-L-lysine-coated cover glasses coated with 0.5% laminin, and incubated for 4 hours at 37°C and 5% CO_2. Stimulation reagents were applied in feeding medium containing 1% penicillin/streptomycin/glutamine, 2% B27, and 0.5 mmol/L GlutaMax in Neurobasal™-A medium. Cultured DEGs were stimulated with 10, 50, or 100 nmol/L EDN1, 6.3 nmol/L IL-31, or medium as vehicle control for the indicated time points. In selected experiments, 100 μmol/L bosentan, or 10 μmol/L U0126, PD98059, SB202190, SP600125, or medium as vehicle control was applied 1 hours before EDN1 stimulation.

2.7 | Immunofluorescence and image analysis

Primary cultured DRG neurons were fixed in 4% paraformaldehyde at room temperature for 10 minutes and permeabilized with 0.2% Triton X-100 in phosphate-buffered saline for 10 minutes. Then, they were blocked with 1% bovine serum albumin and 0.1% Tween 20 in phosphate-buffered saline for 30 minutes. Samples were incubated overnight with anti–βIII-tubulin antibody in blocking solution, and goat anti-mouse IgG (H + L) cross-adsorbed secondary antibody, Alexa Fluor 488, was added for 1 hours. Finally, the cells were mounted with Mounting Medium with DAPI. The total length of all branched structures of dendrites was measured by ImageJ 1.51k.

2.8 | Statistics

All data are presented as mean ± standard error of the mean (SEM). The statistical significance of the differences between values was determined by one-way analysis of variance, followed by Bonferroni's multiple comparison test, using GraphPad PRISM5 software version 5.02. A *P*-value of less than .05 was considered statistically significant.

3 | RESULTS

3.1 | Topical application of endothelin receptor antagonist bosentan alleviates the clinical symptoms of mite-induced dermatitis in NC/Nga mice

As shown previously,[32] the epicutaneous application of mite-antigen in this study appeared to evoke severe dermatitis, ear swelling, and scratching in the AD-ethanol group compared with the status in the control-ethanol group (Figure 1B–E). Topical application of the specific EDNR antagonist bosentan significantly reduced the clinical manifestations (Figure 1B), dermatitis score (Figure 1C), ear thickness (Figure 1D), and scratching behavior (Figure 1E) in the AD-bosentan group compared with those in the AD-ethanol group. Significant differences in dermatitis score were observed between the AD-ethanol group and the AD-bosentan group on days 10, 14, 17, and 21 (Figure 1C) and in ear thickness on days 14, 17, and 21 (Figure 1D). However, in comparison with those in the control-ethanol group, dermatitis score (Figure 1C) and ear thickness (Figure 1D) were still significantly higher in the AD-bosentan group. We also compared the control-ethanol group and the group with bosentan and no mite application, but there were no significant differences in skin manifestations and scratching behavior (data not shown).

3.2 | Topical application of bosentan attenuates the histological changes of mite-antigen–induced dermatitis in mice

Consistent with the clinical scores and scratching behavior, histological analysis of skin samples on day 22 showed more intense inflammatory cell infiltration in AD-ethanol mice than in control-ethanol mice (Figure 2A and B). Topical bosentan significantly reduced the number of dermal inflammatory cells in the AD-bosentan group compared with that in the AD-ethanol group (Figure 2A and B). Significant reduction of the number of infiltrating eosinophils stained with anti-eosinophil cationic protein antibody was also observed in the AD-bosentan group compared with that in the AD-ethanol group (Figure 2C). Moreover, mast cell infiltration visualized by staining with anti-tryptase antibody (Figure 2A) was also significantly decreased in the AD-bosentan group compared with that in the AD-ethanol group (Figure 2D). However, significant infiltration of these cells still remained upon comparison between the control-ethanol group and the AD-bosentan group (Figure 2A–D). We also compared the control-ethanol group and the group with bosentan and no mite application, but there were no significant differences in the dermal infiltration of inflammatory cells, eosinophils, and mast cells (data not shown).

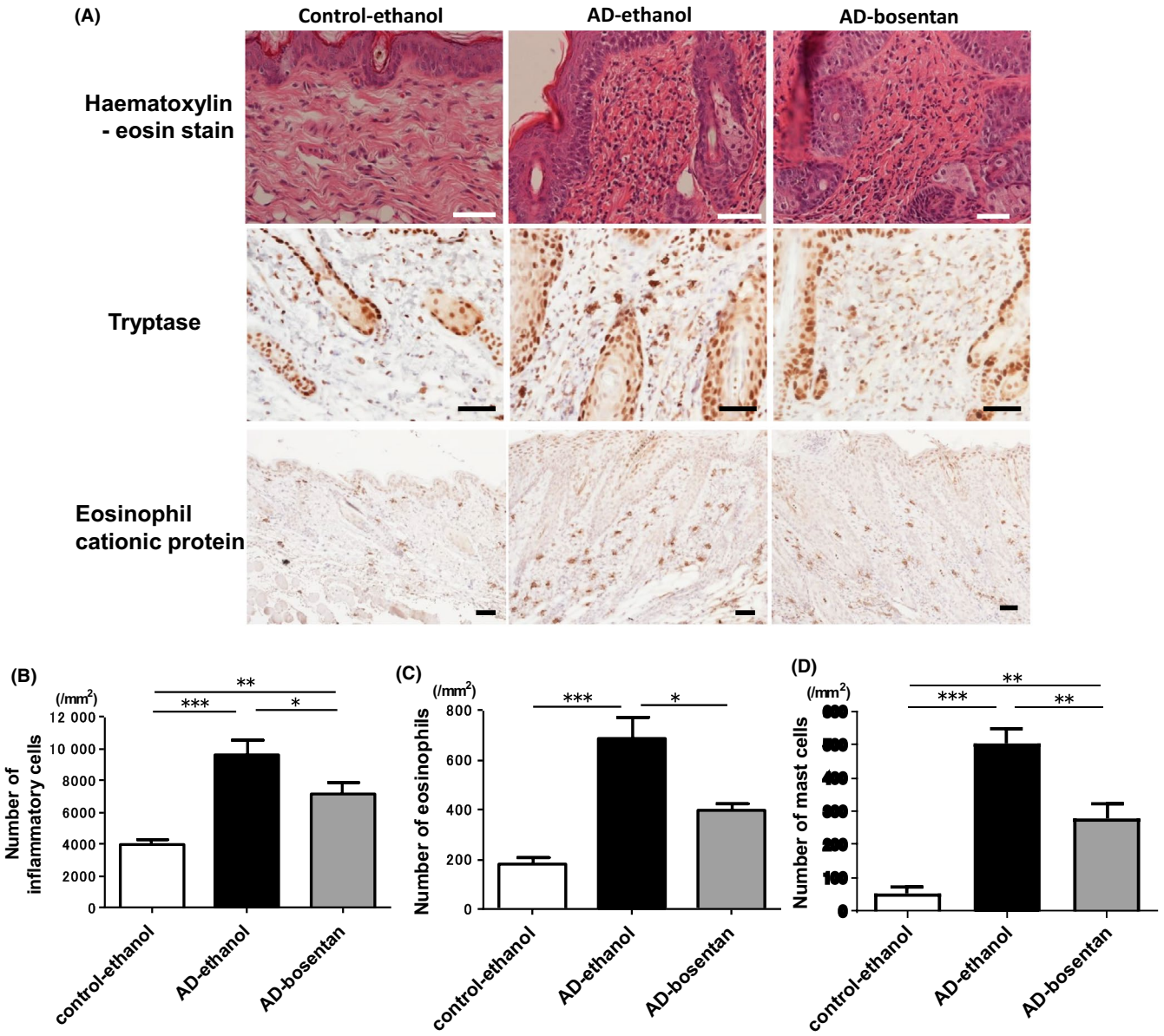

FIGURE 2 Topical application of bosentan histologically improved mite-antigen–induced dermatitis in NC/Nga mice. (A) Histological appearance of skin lesions of control-ethanol, AD-ethanol, and AD-bosentan groups on day 22. Upper, middle, and lower panels show hematoxylin-eosin staining and staining with anti-tryptase antibody and anti-eosinophil cationic protein antibody, respectively. (B–D) Numbers of total inflammatory cells (B), eosinophils (C), and mast cells (D) in the dermis of mice. *$P < .05$, **$P < .01$, ***$P < .001$. Scale bar: 40 μm. Each group consisted of seven mice. Representative data of three independent experiments are shown

3.3 | Topical bosentan inhibits the lesional *Il13*, *Il17a*, and *Ifng* expression and serum TARC and mite-specific IgG levels in AD mice

We next examined the mRNA levels of dermatitis-related cytokines in the lesional skin of AD-like dermatitis with or without bosentan treatment. Skin samples were taken from mite-antigen–treated ear skin, and the mRNA levels of *Il4*, *Il13*, *Il17a*, and *Ifng* were determined by qRT-PCR. In the AD-ethanol group, all of these mRNA levels were significantly increased compared with those in the control-ethanol group. Topical bosentan application significantly decreased the expression of *Il13*, *Il17a*, and *Ifng*, but not that of *Il4* (Figure 3), although *Il13* expression was not completely inhibited by bosentan application. Serum samples were taken from the mice, and TARC, eotaxin, and mite-specific IgG levels were measured by ELISA. Compared with those in the control-ethanol group, the TARC and mite-specific IgG levels in the AD-ethanol group were significantly elevated, but were again significantly inhibited in the AD-bosentan group (Figure 4). Eotaxin in serum was not involved in this mite-induced AD mouse model (Figure 4B). The expression of IL-25 was immunohistologically strongly augmented throughout all epidermal layers in the AD-ethanol group (Figure S1A). The epidermal IL-25 expression was significantly inhibited to almost the same level as the control by topical bosentan (Figure S1B).

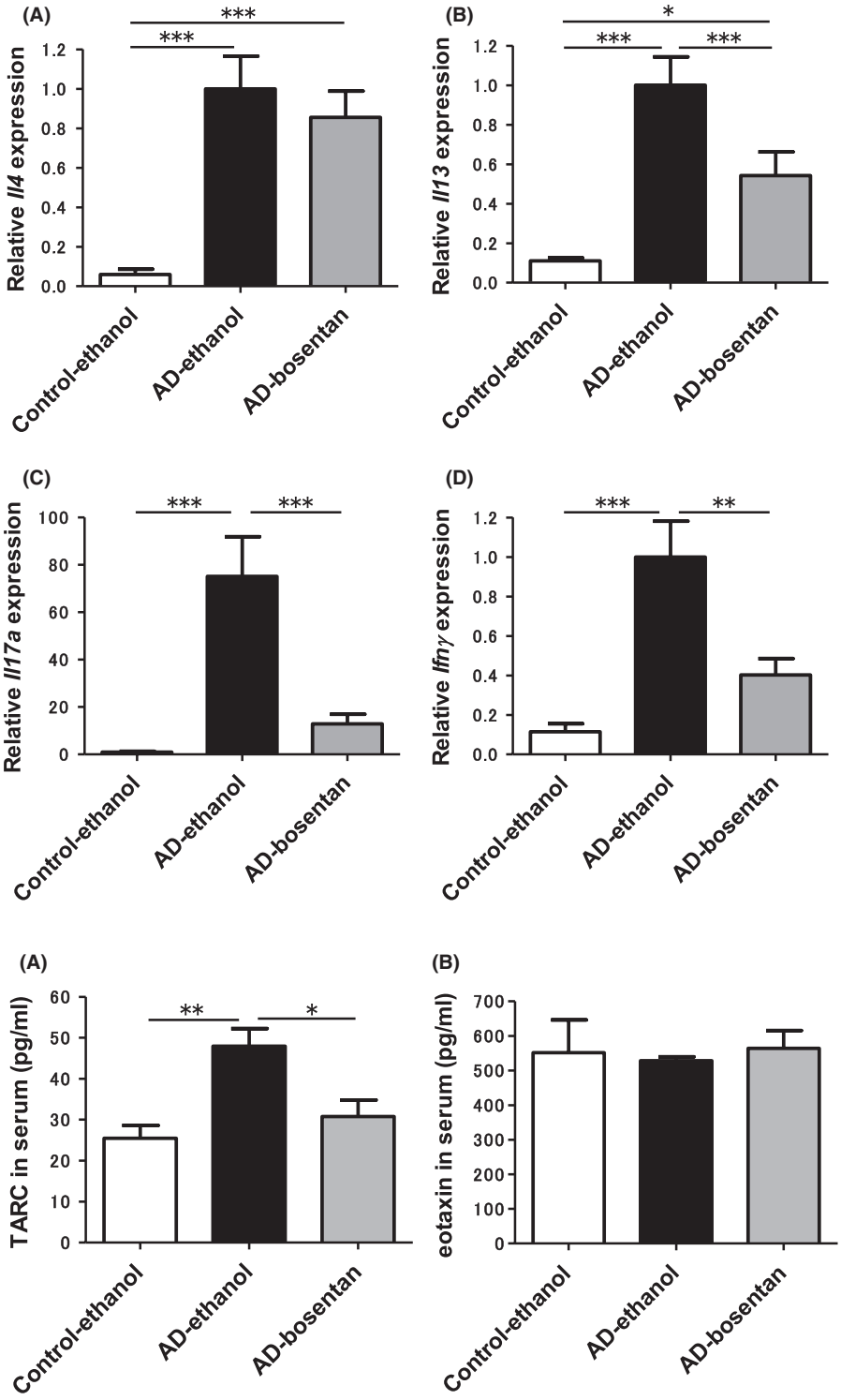

FIGURE 3 Topical bosentan inhibits the lesional *Il13*, *Il17a*, and *Ifng* expression in AD mice. (A) IL-4, (B) IL-13, (C) IL-17, and (D) IFN-γ mRNA levels were analyzed by real-time PCR in ear skin of NC/Nga mice. $^{*}P < .05$, $^{**}P < .01$, $^{***}P < .001$. Each group consisted of seven mice. Representative data of three independent experiments are shown

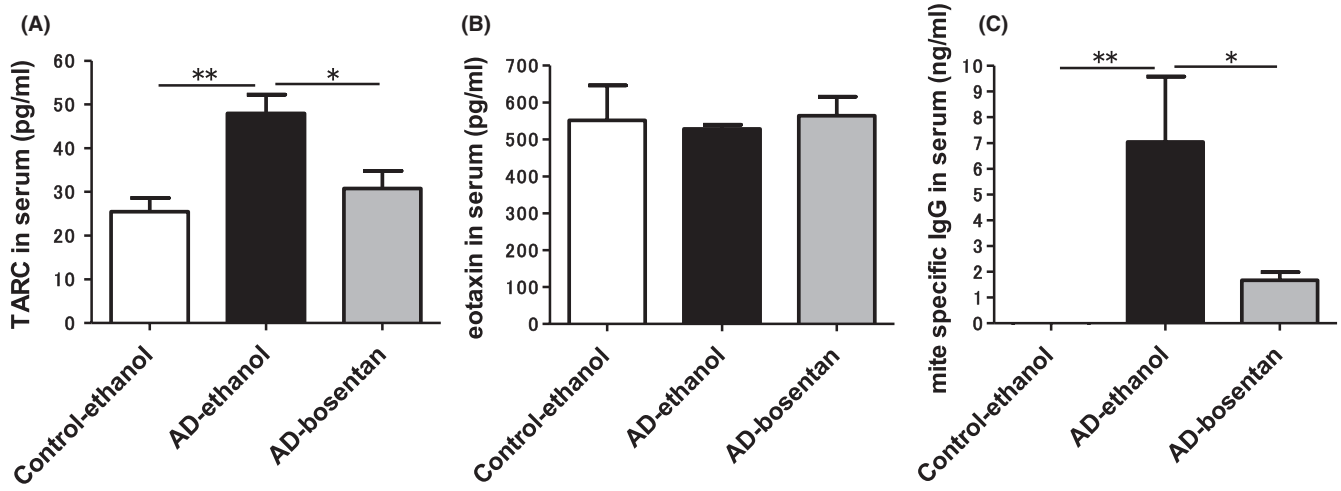

FIGURE 4 Increases of serum TARC levels and mite-specific IgG in AD mice were suppressed by bosentan. Serum TARC (A), eotaxin (B), and mite-specific IgG levels (C) in mice were measured by ELISA. $^{*}P < .05$, $^{**}P < .01$. Each group consisted of seven mice. Representative data of three independent experiments are shown

3.4 | Topical bosentan inhibits epidermal EDN1 expression and the number of intraepidermal nerve fibers

Although the expression of EDN1 was immunohistologically confined to the lower part of the epidermis in the control-ethanol group, it was strongly augmented throughout all epidermal layers in the AD-ethanol group (Figure 5A), as was previously reported.[24] Notably, the epidermal EDN1 expression appeared to be inhibited to the same level as in the control by the topical bosentan (Figure 5A). As bosentan inhibited pruritus/scratching in the present experiments, we next measured the number of

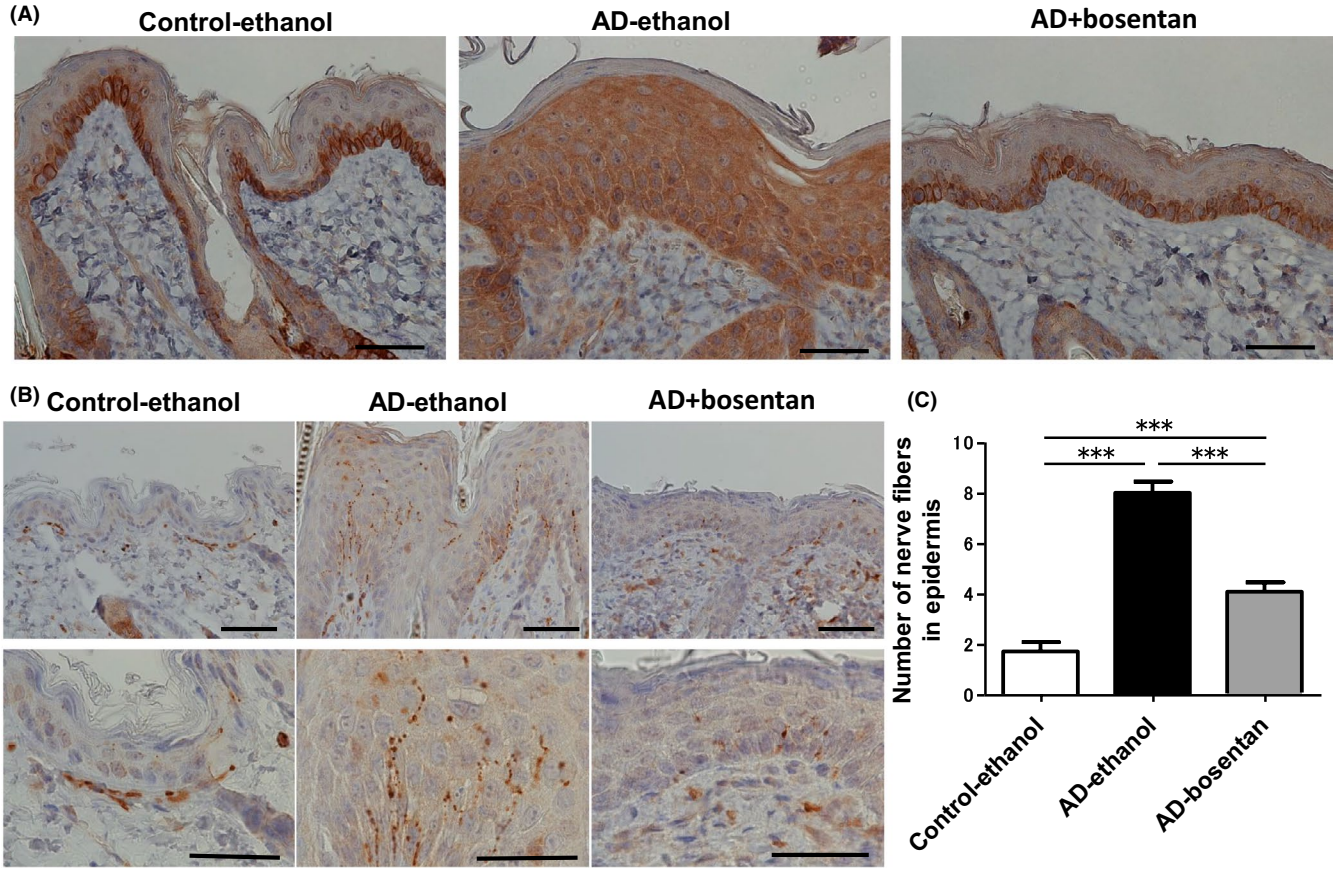

FIGURE 5 Topical bosentan suppresses the augmentation of epidermal EDN1 expression and intraepidermal nerve fibers in AD mice. (A) Immunohistochemical staining for EDN1 of skin lesions of control-ethanol, AD-ethanol, and AD-bosentan groups. (B) Representative images of PGP9.5-positive nerves in back skin of mice. (C) The number of intradermal PGP9.5-positive nerves was counted and calculated per high-power field. ***$P < .001$. Scale bar: 40 μm. Each group consisted of seven mice. Representative data of three independent experiments are shown

epidermal nerve fibers by PGP9.5 immunostaining. In the AD-ethanol group, the number of epidermal nerve fibers was significantly increased compared with that in the control-ethanol group (Figure 5B and C). Topical bosentan application significantly reduced the number of epidermal nerve fibers in AD-bosentan mice compared with that in AD-ethanol mice, but there was not a complete reduction to the level in the control-ethanol group (Figure 5B and C).

3.5 | EDN1 promotes neuronal elongation and branching in small-diameter DRG neurons, which is inhibited by bosentan

As the number of epidermal nerve fibers was increased in the EDN1-rich epidermis (Figure 5), we next analyzed the effects of EDN1 on DRG neurons. We used cultured dissociated DRG neurons that we treated with IL-31 (which has attracted attention as a pruritogen in patients with AD),[7] EDN1, or vehicle control for 24 hours. Regarding the pruritogen IL-31,[7] Feld et al recently reported that it promoted the growth of sensory nerves in vitro and in vivo.[33] In DRG neurons with a small diameter (≤20 μm), EDN1 and IL-31 induced neurite elongation and branch formation compared with the status of neurons treated with vehicle control (Figure 6A and B). Interestingly, both EDN1 and IL-31 affected neither neurite elongation nor branch formation in large-diameter DRG neurons (>20 μm) (Figure S2). Small-diameter DRG cells were stimulated with 0-100 nmol/L EDN1. As shown in Figure S3, both neurite elongation and branch formation were significantly upregulated in DRG neurons by EDN1, with an optimal dose of approximately 50 nmol/L. The neurostimulatory effects of EDN1 were shown to occur in an incubation time-dependent manner (Figure S2). Bosentan significantly inhibited the EDN1-induced neurite elongation and branch formation of small-diameter DRG neurons (Figure 6C). We finally examined the cell signaling associated with the neurostimulatory effects of EDN1 and focused on the MAPK pathway, one of the signaling pathways related to the EDN. The EDN1-mediated upregulation of neurite elongation and branch formation in small-diameter DRG neurons was completely abrogated by the p38 MAPK inhibitor SB202190 and the JNK inhibitor SP600125, but not by the ERK1/2 inhibitor U0126 or the MEK1/2 inhibitor PD98059 (Figure S4). Interestingly, baseline neurite elongation and branch formation were rather augmented by U0126 or PD98059 (FigureS4).

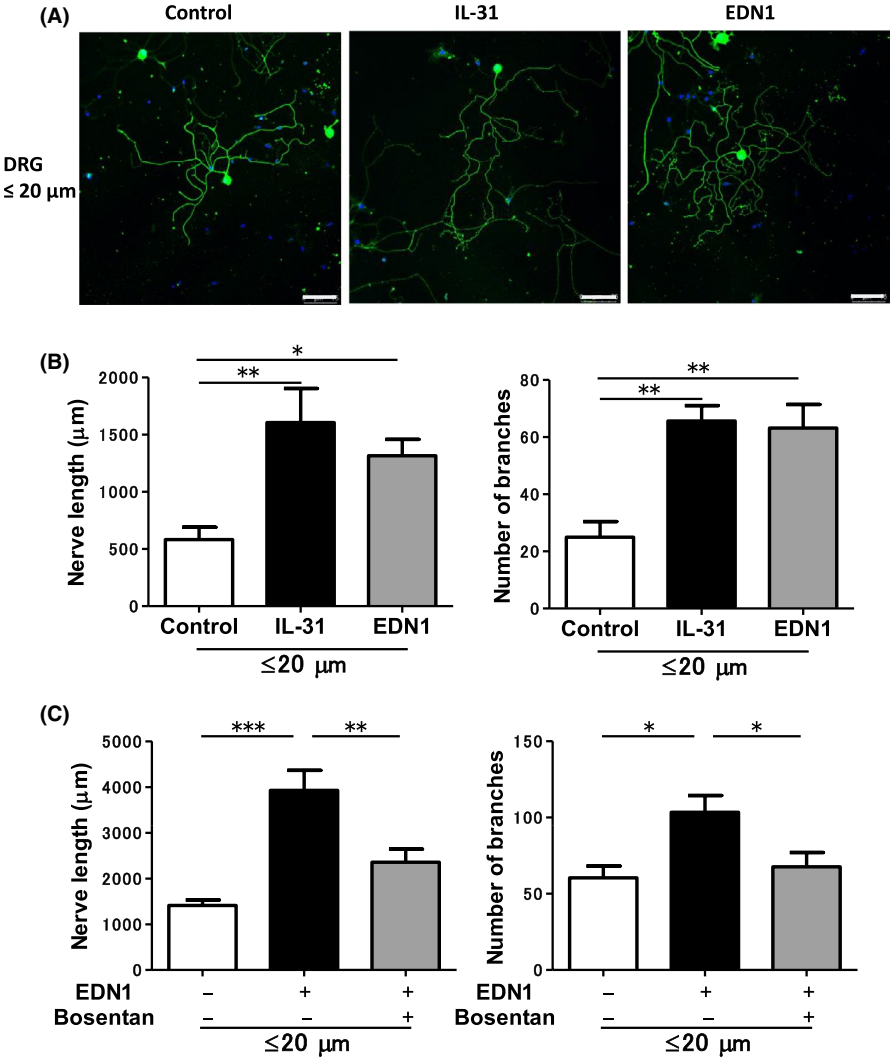

FIGURE 6 EDN1 induces neurite elongation and branching in small-diameter DRG neurons, which is inhibited by bosentan. (A) Neurite outgrowth from small-diameter (≤20 µm) DRG neurons stimulated with EDN1, IL-31, or control medium. (B) Quantification of the neurite length and branching in small-diameter DRG neurons incubated with control medium, IL-31 (100 ng/ml), or EDN1 (50 nmol/L) for 24 h (n = 6-10). (C) Small-diameter DRG neurons were stimulated with EDN1 (50 nmol/L) alone or control medium for 24 h. Bosentan (100 µmol/L) or control medium was applied 1 h before EDN1 stimulation (n = 8-11). *$P < .05$, **$P < .01$, ***$P < .001$. Scale bar: 75 µm. Representative data of three independent experiments are shown

4 | DISCUSSION

Although EDN1 induces pruritus and might be involved in chronic AD inflammation,[7] the effects of EDNR blockade on AD remain unresolved. Here, we report for the first time that topical application of the EDNR antagonist bosentan efficiently reduced skin inflammation, pruritus, and the number of intraepidermal nerve fibers of the mite-antigen–induced AD-like murine model.

This AD-like murine model used in this study mimics human AD. The lesional skin in AD mice manifests erythema, scaling, and lichenification with itching/scratching behavior.[32] In the present study, we also found elevated plasma TARC levels, upregulated expression of epidermal EDN1, and an increased number of intraepidermal nerve fibers. Blockade of EDNR by bosentan significantly alleviated the clinical dermatitis scores, ear thickness, and itching/scratching behavior. In parallel with this, bosentan attenuated the infiltration of inflammatory cells (eosinophils and mast cells) in the lesional dermis. Plasma TARC levels were also downregulated by topical bosentan. These anti-inflammatory effects of bosentan have been reported in previous studies. For example, bosentan was previously reported to reduce the release of secondary mediators such as IL-1, IL-6, IL-8, and tumor necrosis factor-α (TNF-α) produced by monocytes stimulated with endothelin.[30,31] It could also inhibit the upregulation of cell adhesion molecules on the endothelium and leukocytes such as neutrophils and T cells.[34-36] Furthermore, the effectiveness of bosentan has been reported in several mouse or rat disease models. For example, in an ovalbumin-induced allergic rhinitis rat model, oral bosentan significantly inhibited nasal symptoms and serum IgE level.[37] In addition, in a murine model of inflammatory bowel disease and a rat colitis model, bosentan significantly reduced clinical and histological inflammation.[38,39] Moreover, in rat models of airway inflammation, bosentan also reduced the levels of eosinophils and several cytokines including IL-4, TNF-α, IFN-γ, and IL-1β in bronchoalveolar lavage fluid and lung inflammation.[40,41] These results suggest that bosentan has a sufficient anti-inflammatory effect and that its topical application could potentially be used for protective drugs against AD. Further examinations will be required to determine whether it can be used as a therapeutic agent for AD and how effective bosentan is compared to other topical products such as topical corticosteroid or tacrolimus ointment. Furthermore,

this study was only performed in one AD mouse model. Since atopic dermatitis is a multifactorial disease, further studies will be needed to reveal its relationship to other factors.

While multiple molecules have been implicated in AD, studies in mice and humans have elucidated central roles of IL-4 and IL-13.[42,43] The essential role of the type 2 axis was confirmed by the clinical success of dupilumab, an anti–IL-4Rα antibody that modulates the signaling of both IL-4 and IL-13 pathways.[44] In the present study, bosentan significantly suppressed mRNA of *Il13*, *Il17*, and *Ifng* but not *Il4* in the analysis of cytokine expression in the skin. Bosentan application significantly suppressed the dermatitis and pruritus in the mite-induced AD mouse model even though it did not suppress IL-4 expression in the skin, which would indicate that IL-13 plays a greater role than IL-4 in this mite-induced AD mouse model. In fact, it has been reported that two anti–IL-13 antibodies, tralokinumab and lebrikizumab, were effective in a phase 2 clinical trial of AD.[45,46] Gene expression studies in AD patients also suggested that IL-13 might be of particular pathophysiological importance.[47] However, in the present study, bosentan did not completely abrogate the inflammation and pruritus of the mite-induced mouse model. In regard to the relative efficacy of biologics, it was reported that the strongest evidence is currently available for dupilumab, which modulates the signaling of both IL-4 and IL-13 pathways.[48] These results suggest that IL-13 may be more important but IL-4 would also be involved in the inflammation of AD.

In the present study, blockade of EDNR by bosentan abrogated the mRNA expression of *Il13*, *Il17*, and *Ifng*, but not *Il4*. This might be consistent with the fact that EDN1 induces the release of IL-25 in keratinocytes as we showed previously[48] and in Figure S1, and IL-25 induces the activation of ILC2, which releases high levels of IL-13, IL-5, and IL-9, but not IL-4.[25] Further investigations will be needed to determine whether ILC2 increases in this AD mouse model and whether blockade of EDNR by bosentan can inhibit ILC2 infiltration through IL-25 suppression.

The density of epidermal nerve fibers is higher in the skin of patients with AD than in that of healthy controls; this has been suggested to be partly responsible for the hyperkinesis—a state of hypersensitivity of the itch sensation—seen in these patients.[49-51] As the epidermal EDN1 expression was augmented with an increased number of lesional intraepidermal nerve fibers, which were significantly inhibited by topical bosentan, we assumed that EDN1 might affect neuronal growth. Therefore, we next examined the effects of EDN1 and bosentan in DRG neurons. EDN1 potently accelerated the neuronal elongation and branching of DRG cells, which were effects similar to those of IL-31, a pruritogen reported to promote the growth of sensory nerves in vitro and in vivo.[33] EDNR blockade with bosentan abrogated the nerve length and number of branches of DRG by EDN1, as expected. The EDN1-mediated neurostimulatory effects were evident only in small-diameter (<20 μm) DRG cells, but not in large-diameter ones. Similar neurostimulatory effects have been reported for IL-31 and histamine, which are related to the pathogenesis of atopic inflammation and itch.[33,52,53] Specifically, the pruritogenic IL-31 and histamine have been shown to upregulate the neurite elongation of small-diameter DRG neurons.[33,53] These results reinforce the assertion that EDN1 is a plausible candidate to be included among these itch-related mediators in the pathogenesis of AD.

Interestingly, in the present study, nerve elongation was augmented by EDN1 in a dose-dependent manner up to 100 nmol/L, while the increase of branching peaked at 50 nmol/L and was not observed at 100 nmol/L. Recently, intensive research has focused on understanding the mechanisms of outgrowth and branching of neurons.[54-56] In particular, several glycerophospholipids and several of their interacting proteins are involved in the elongation and branching of neurons.[57] It has been found that different specific lipids are needed in the extension and branching of neurons. The heterogeneous responsiveness of nerve elongation and branching to EDN1 in this study might have been caused by the differences in mechanisms between nerve elongation and branching. However, the precise mechanisms of the preventive effects of bosentan in the AD-like mouse model and on epidermal innervation are not fully understood. Further investigation is warranted to explore the subcellular molecular mechanisms involved.

The EDN1-induced neurostimulatory effects were dependent on the p38 MAPK and JNK, but not MEK/ERK, pathways. Previous studies reported that IL-31–induced neuronal outgrowth was mediated via the activation of signal transducer and activator of transcription 3[33] and that histamine-induced neurite outgrowth was possibly mediated by the protein kinase Cδ-mediated cell signaling pathway.[53] It has been reported that the JNK, p38 MAPK, and MEK/ERK pathways are differentially involved in neurite growth and branching in a stimulus-dependent manner.[58-61] Further investigation is warranted to clarify the signaling pathways leading to neuronal elongation and branching in peripheral nerves.

In conclusion, our study revealed that the topical application of bosentan efficiently reduced the mite-induced dermatitis, itching/scratching, intraepidermal nerve fibers, epidermal EDN1 expression, and circulating TARC levels in a murine AD model. EDN1 potently accelerated the nerve elongation and branching in small-diameter DRG neurons, which was significantly inhibited by the EDNR antagonist bosentan. Considering the pruritogenic activity of EDN1 in mice and humans,[19-21] the EDN1/EDNR system should be better integrated into our understanding of the pathogenesis of AD. Moreover, EDNR blockade is a potential therapeutic target for AD.

CONFLICTS OF INTEREST

The authors declare that they have no conflict of interest.

ORCID

Makiko Kido-Nakahara https://orcid.org/0000-0002-4169-1309
Gaku Tsuji https://orcid.org/0000-0003-1472-1864
Masutaka Furue https://orcid.org/0000-0002-2967-1073
Takeshi Nakahara https://orcid.org/0000-0003-2811-8273

REFERENCES

1. Bieber T. Atopic dermatitis 2.0: from the clinical phenotype to the molecular taxonomy and stratified medicine. *Allergy*. 2012;67:1475-1482.

2. Furue M, Chiba T, Tsuji G, et al. Atopic dermatitis: immune deviation, barrier dysfunction, IgE autoreactivity and new therapies. *Allergol Int*. 2017;66:398-403.
3. Saeki H, Nakahara T, Tanaka A, et al. Clinical Practice Guidelines for the Management of Atopic Dermatitis 2016. *J Dermat*. 2016;43(10):1117-1145.
4. Pavlis J, Yosipovitch G. Management of itch in atopic dermatitis. *Am J Clin Dermatol*. 2018;19:319-332.
5. Werfel T, Allam JP, Biedermann T, et al. Cellular and molecular immunologic mechanisms in patients with atopic dermatitis. *J Allergy Clin Immunol*. 2016;138:336-349.
6. Hradetzky S, Werfel T, Rösner LM. Autoallergy in atopic dermatitis. *Allergo J Int*. 2015;24:16-22.
7. Kido-Nakahara M, Furue M, Ulzii D, Nakahara T. Itch in atopic dermatitis. *Immunol Allergy Clin North Am*. 2017;37:113-122.
8. Yanagisawa M, Kurihara H, Kimura S, et al. A novel potent vasoconstrictor peptide produced by vascular endothelial cells. *Nature*. 1988;332:411-415.
9. Tsuboi R, Sato C, Oshita Y, et al. Ultraviolet B irradiation increases endothelin-1 and endothelin receptor expression in cultured human keratinocytes. *FEBS Lett*. 1995;371:188-190.
10. Maurer M, Wedemeyer J, Metz M, et al. Mast cells promote homeostasis by limiting endothelin-1-induced toxicity. *Nature*. 2004;432:512-516.
11. Spirig R, Potapova I, Shaw-Boden J, Tsui J, Rieben R, Shaw SG. TLR2 and TLR4 agonists induce production of the vasoactive peptide endothelin-1 by human dendritic cells. *Mol Immunol*. 2009;46:3178-3182.
12. Ehrenreich H, Anderson RW, Fox CH, et al. Endothelins, peptides with potent vasoactive properties, are produced by human macrophages. *J Exp Med*. 1990;172:1741-1748.
13. Guruli G, Pflug BR, Pecher S, Makarenkova V, Shurin MR, Nelson JB. Function and survival of dendritic cells depend on endothelin-1 and endothelin receptor autocrine loops. *Blood*. 2004;104:2107-2115.
14. Elferink JG, de Koster BM. Endothelin-induced activation of neutrophil migration. *Biochem Pharmacol*. 1994;48:865-871.
15. Bagnato A, Venuti A, Di Castro V, Marcante ML. Identification of the ETA receptor subtype that mediates endothelin induced autocrine proliferation of normal human keratinocytes. *Biochem Biophys Res Commun*. 1995;209:80-86.
16. Olender J, Nowakowska-Zajdel E, Walkiewicz K, Muc-Wierzgoń M. Endothelins and carcinogenesis. *Postepy Hig Med Dosw*. 2016;70:872-880.
17. Soldano S, Montagna P, Villaggio B, et al. Endothelin and sex hormones modulate the fibronectin synthesis by cultured human skin scleroderma fibroblasts. *Ann Rheum Dis*. 2009;68:599-602.
18. Goldie RG, Henry PJ. Endothelins and asthma. *Life Sci*. 1999;65:1-15.
19. Trentin PG, Fernandes MB, D'Orleans-Juste P, Rae GA. Endothelin-1 causes pruritus in mice. *Exp Biol Med*. 2006;231:1146-1151.
20. Gomes LO, Hara DB, Rae GA. Endothelin1 induces itch and pain in the mouse cheek model. *Life Sci*. 2012;91:628-633.
21. Kido-Nakahara M, Buddenkotte J, Kempkes C, et al. Neural peptidase endothelin-converting enzyme 1 regulates endothelin 1-induced pruritus. *J Clin Invest*. 2014;124:2683-2695.
22. Akiyama T, Carstens E. Neural processing of itch. *Neuroscience*. 2013;250:697-714.
23. Tsybikov NN, Petrisheva IV, Kuznik BI, Magen E. Plasma endothelin-1 levels during exacerbation of atopic dermatitis. *Allergy Asthma Proc*. 2015;36:320-324.
24. Aktar MK, Kido-Nakahara M, Furue M, Nakahara T. Mutual upregulation of endothelin-1 and IL-25 in atopic dermatitis. *Allergy*. 2015;70:846-854.
25. Salimi M, Barlow JL, Saunders SP, et al. A role for IL-25 and IL-33-driven type-2 innate lymphoid cells in atopic dermatitis. *J Exp Med*. 2013;210:2939-2950.
26. Nakahara T, Kido-Nakahara M, Ohno F, et al. The pruritogenic mediator endothelin-1 shifts the dendritic cell-T-cell response toward Th17/Th1 polarization. *Allergy*. 2018;73:511-515.
27. Kedzierski RM, Yanagisawa M. Endothelin system: the double-edged sword in health and disease. *Annu Rev Pharmacol Toxicol*. 2001;41:851-876.
28. Sandoval YH, Atef ME, Levesque LO, Li Y, Anand-Srivastava MB. Endothelin-1 signaling in vascular physiology and pathophysiology. *Curr Vasc Pharmacol*. 2014;12:202-214.
29. Véniant M, Clozel JP, Hess P, Clozel M. Endothelin plays a role in the maintenance of blood pressure in normotensive guinea pigs. *Life Sci*. 1994;55(6):445-454.
30. Cunningham ME, Huribal M, Bala RJ, McMillen MA. Endothelin-1 and endothelin-4 stimulate monocyte production of cytokines. *Crit Care Med*. 1997;25:958-964.
31. McMillen MA, Huribal M, Kumar R, Sumpio BE. Endothelin-stimulated human monocytes produce prostaglandin E2 but not leukotriene B4. *J Surg Res*. 1993;54:331-335.
32. Yamamoto M, Haruna T, Yasui K, et al. A novel atopic dermatitis model induced by topical application with *Dermatophagoides farinae* extract in NC/Nga mice. *Allergol Int*. 2007;56:139-148.
33. Feld M, Garcia R, Buddenkotte J, et al. The pruritus- and TH2-associated cytokine IL-31 promotes growth of sensory nerves. *J Allergy Clin Immunol*. 2016;138(2):500-508.
34. Zouki C, Baron C, Fournier A, Filep JG. Endothelin-1 enhances neutrophil adhesion to human coronary artery endothelial cells: role of ET(A) receptors and platelet-activating factor. *Br J Pharmacol*. 1999;127:969-979.
35. Verma S, Li SH, Badiwala MV, et al. Endothelin antagonism and interleukin-6 inhibition attenuate the proatherogenic effects of C-reactive protein. *Circulation*. 2002;105:1890-1896.
36. Iannone F, Riccardi MT, Guiducci S, et al. Bosentan regulates the expression of adhesion molecules on circulating T cells and serum soluble adhesion molecules in systemic sclerosis-associated pulmonary arterial hypertension. *Ann Rheum Dis*. 2008;67:1121-1126.
37. Tatar A, Yayla M, Kose D, Halici Z, Yoruk O, Polat E. The role of endothelin-1 and endothelin receptor antagonists in allergic rhinitis inflammation: ovalbumin-induced rat model. *Rhinology*. 2016;54:266-272.
38. Anthoni C, Mennigen RB, Rijcken EJ, et al. Bosentan, an endothelin receptor antagonist, reduces leucocyte adhesion and inflammation in a murine model of inflammatory bowel disease. *Int J Colorectal Dis*. 2006;21:409-418.
39. Hogaboam CM, Muller MJ, Collins SM, Hunt RH. An orally active non-selective endothelin receptor antagonist, bosentan, markedly reduces injury in a rat model of colitis. *Eur J Pharmacol*. 1996;309:261-269.
40. Finsnes F, Lyberg T, Christensen G, Skjønsberg OH. Effect of endothelin antagonism on the production of cytokines in eosinophilic airway inflammation. *Am J Physiol Lung Cell Mol Physiol*. 2001;280:L659-665.
41. Finsnes F, Skjønsberg OH, Tønnessen T, Naess O, Lyberg T, Christensen G. Endothelin production and effects of endothelin antagonism during experimental airway inflammation. *Am J Respir Crit Care Med*. 1997;155:1404-1412.
42. Silverberg JI, Kantor R. The role of interleukins 4 and/or 13 in the pathophysiology and treatment of atopic dermatitis. *Dermatol Clin*. 2017;35:327-334.
43. Moyle M, Cevikbas F, Harden JL, Guttman-Yassky E. Understanding the immune landscape in atopic dermatitis: The era of biologics and emerging therapeutic approaches. *Exp Dermatol*. 2019;28:756-768.
44. Gooderham MJ, Hong HC, Eshtiaghi P, Papp KA. Dupilumab: A review of its use in the treatment of atopic dermatitis. *J Am Acad Dermatol*. 2018;78(3 Suppl 1):S28-S36.

45. Wollenberg A, Howell MD, Guttman-Yassky E, et al. Treatment of atopic dermatitis with tralokinumab, an anti-IL-13 mAb. *J Allergy Clin Immunol*. 2019;143:135-141.
46. Simpson EL, Flohr C, Eichenfield LF, et al. Efficacy and safety of lebrikizumab (an anti-IL-13 monoclonal antibody) in adults with moderate-to-severe atopic dermatitis inadequately controlled by topical corticosteroids: A randomized, placebo-controlled phase II trial (TREBLE). *J Am Acad Dermatol*. 2018;78(5):863-871.
47. Tazawa T, Sugiura H, Sugiura Y, Uehara M. Relative importance of IL-4 and IL-13 in lesional skin of atopic dermatitis. *Arch Dermatol Res*. 2004;295:459-464.
48. Seger EW, Wechter T, Strowd L, Feldman SR. Relative efficacy of systemic treatments for atopic dermatitis. *J Am Acad Dermatol* 2019;80: 411-416.
49. Sugiura H, Omoto M, Hirota Y, Danno K, Uehara M. Density and fine structure of peripheral nerves in various skin lesions of atopic dermatitis. *Arch Dermatol Res*. 1997;289:125-131.
50. Tobin D, Nabarro G, de la Faute HB, van Vloten WA, van der Putte SCJ, Schuurman H-J. Increased number of immunoreactive nerve fibers in atopic dermatitis. *J Allergy Clin Immunol*. 1992;90:613-622.
51. Tominaga M, Takamori K. Itch and nerve fibers with special reference to atopic dermatitis: therapeutic implications. *J Dermatol*. 2014;41:205-212.
52. Cevikbas F, Wang X, Akiyama T, et al. A sensory neuron-expressed IL-31 receptor mediates T helper cell-dependent itch: Involvement of TRPV1 and TRPA1. *J Allergy Clin Immunol*. 2014;133:448-460.
53. Inami Y, Sato A, Ohtsu H, et al. Deficiency of histidine decarboxylase attenuates peripheral nerve fibre elongation into the epidermis in surfactant-treated mouse skin. *Exp Dermatol*. 2017;26:441-443.
54. Ammar MR, Kassas N, Bader MF, Vitale N. Phosphatidic acid in neuronal development: A node for membrane and cytoskeleton rearrangements. *Biochimie*. 2014;107:51-57.
55. Paoletti L, Elena C, Domizi P, Banchio C. Role of phosphatidylcholine during neuronal differentiation. *IUBMB Life*. 2011;63:714-720.
56. Ziegler AB, Thiele C, Tenedini F, et al. Cell-autonomous control of neuronal dendrite expansion via the fatty acid synthesis regulator SREBP. *Cell Rep*. 2017;21:3346-3353.
57. Ziegler AB, Tavosanis G. Glycerophospholipids - Emerging players in neuronal dendrite branching and outgrowth. *Dev Biol*. 2019;451:25-34.
58. Lindwall C, Dahlin L, Lundborg G, Kanje M. Inhibition of c-Jun phosphorylation reduces axonal outgrowth of adult rat nodose ganglia and dorsal root ganglia sensory neurons. *Mol Cell Neurosci*. 2004;27:267-279.
59. Raivich G, Bohatschek M, Da Costa C, et al. The AP-1 transcription factor c-Jun is required for efficient axonal regeneration. *Neuron*. 2004;43:57-67.
60. Michaelevski I, Segal-Ruder Y, Rozenbaum M, et al. Signaling to transcription networks in the neuronal retrograde injury response. *Sci Signal*. 2010;3:ra53.
61. Price RD, Yamaji T, Matsuoka N. FK506 potentiates NGF-induced neurite outgrowth via the Ras/Raf/MAP kinase pathway. *Br J Pharmacol*. 2003;140:825-829.

SUPPORTING INFORMATION

Additional supporting information may be found online in the Supporting Information section.

How to cite this article: Kido-Nakahara M, Wang B, Ohno F, et al. Inhibition of mite-induced dermatitis, pruritus, and nerve sprouting in mice by the endothelin receptor antagonist bosentan. *Allergy*. 2020;00:1–11. https://doi.org/10.1111/all.14451

Supplementary Fig. S1. Topical bosentan suppresses the augmentation of epidermal IL-25 expression. (A) Immunohistochemical staining for IL-25 of skin lesions of control-ethanol, AD-ethanol, and AD-bosentan groups. (B) Semi-quantitative assessment of the expression was performed according to the following criteria: no staining: 0 points; weakly positive: 1 point; moderately positive: 2 points; and strongly positive: 3 points. Data are shown as the mean ± SEM. Scale bar: 40 μm. Each group consisted of seven mice. Representative data of three independent experiments are shown.

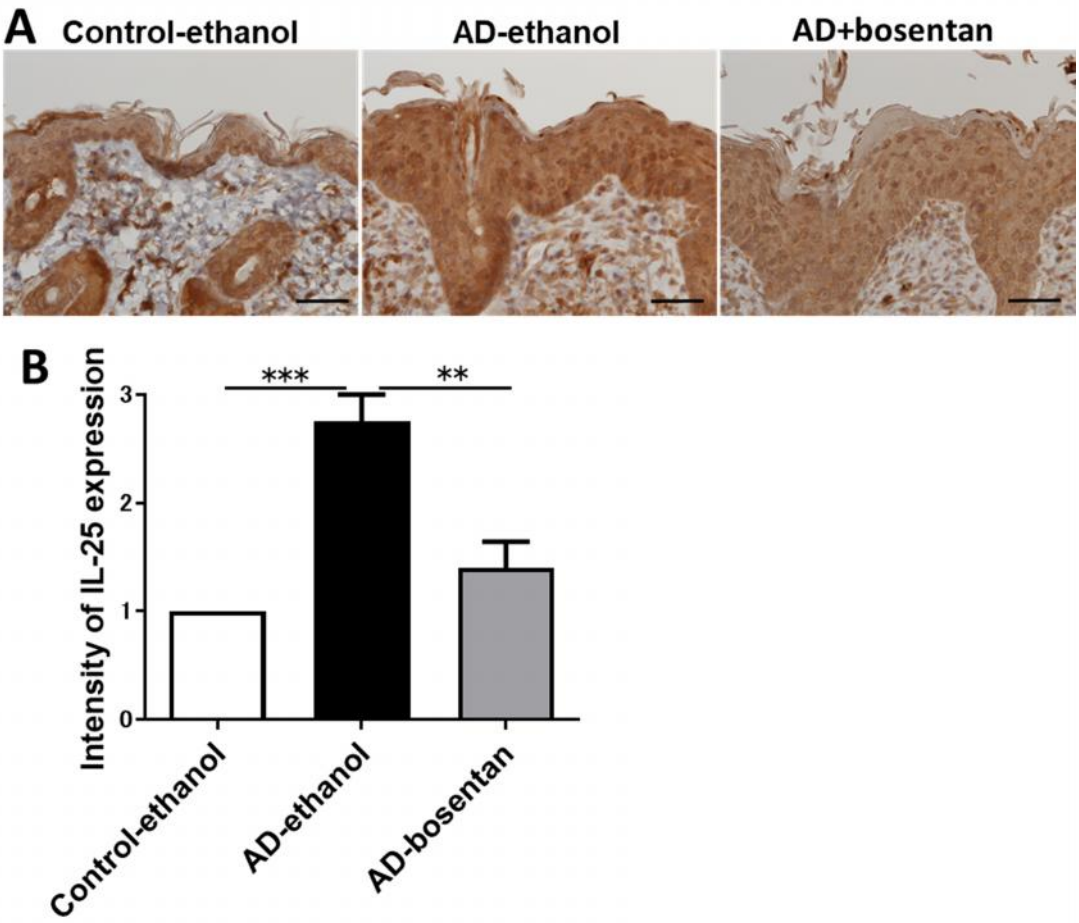

Supplementary Fig. S2. Neurite elongation and branching in large-diameter DRG neurons. (A) Neurite outgrowth from large-diameter (>20 µm) DRG neurons stimulated with EDN1 (50 nM), IL-31 (100 ng/ml), or control medium. (B) Quantification of the neurite length and branching in large-diameter DRG neurons incubated with control medium, IL-31 (100 ng/ml), or EDN1 (50 nM) for 24 h (n=6–10). Data are shown as the mean ± SEM. Scale bar: 75 µm.

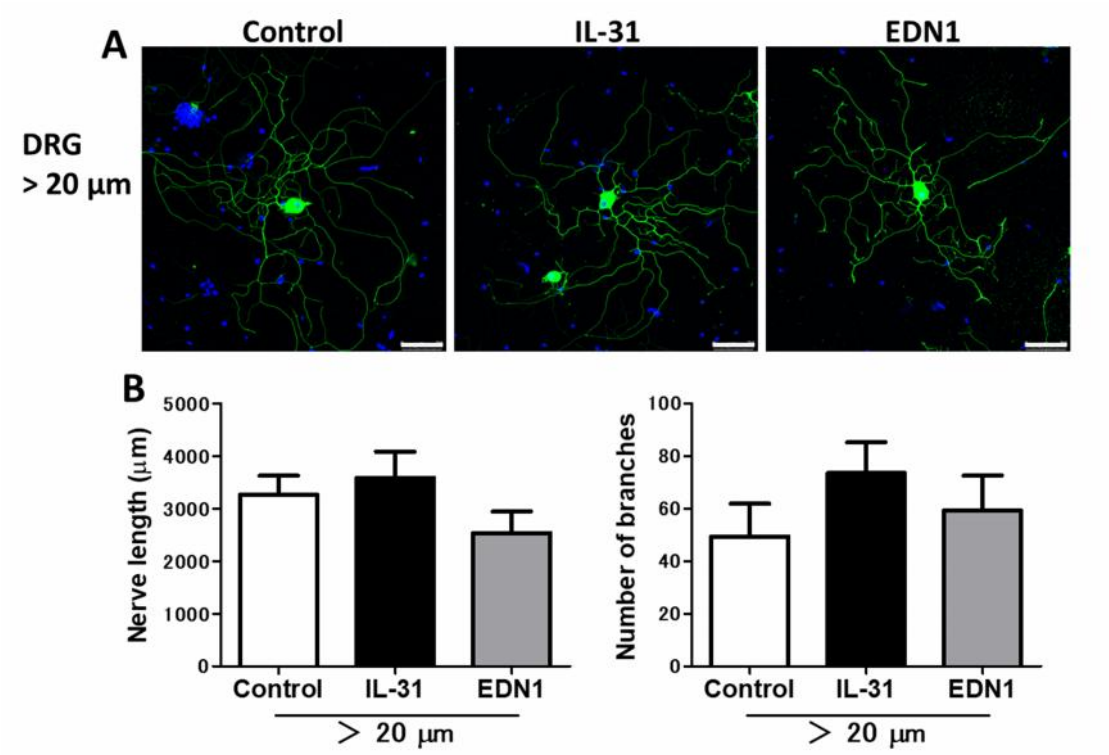

Supplementary Fig. S3. Neurite elongation and branching in small-diameter DRG neurons. (A) Small-diameter (≤20 μm) DRG neurons are stimulated with 0, 10, 50, and 100 nM EDN1 for 24 h (n=8–11). (B) Small-diameter DRG neurons are stimulated with or without EDN1 (50 nM) for 15, 20, 24, and 33 h (n=8–10). Data are shown as the mean ± SEM. *p<0.05, **p<0.01, ***p<0.001.

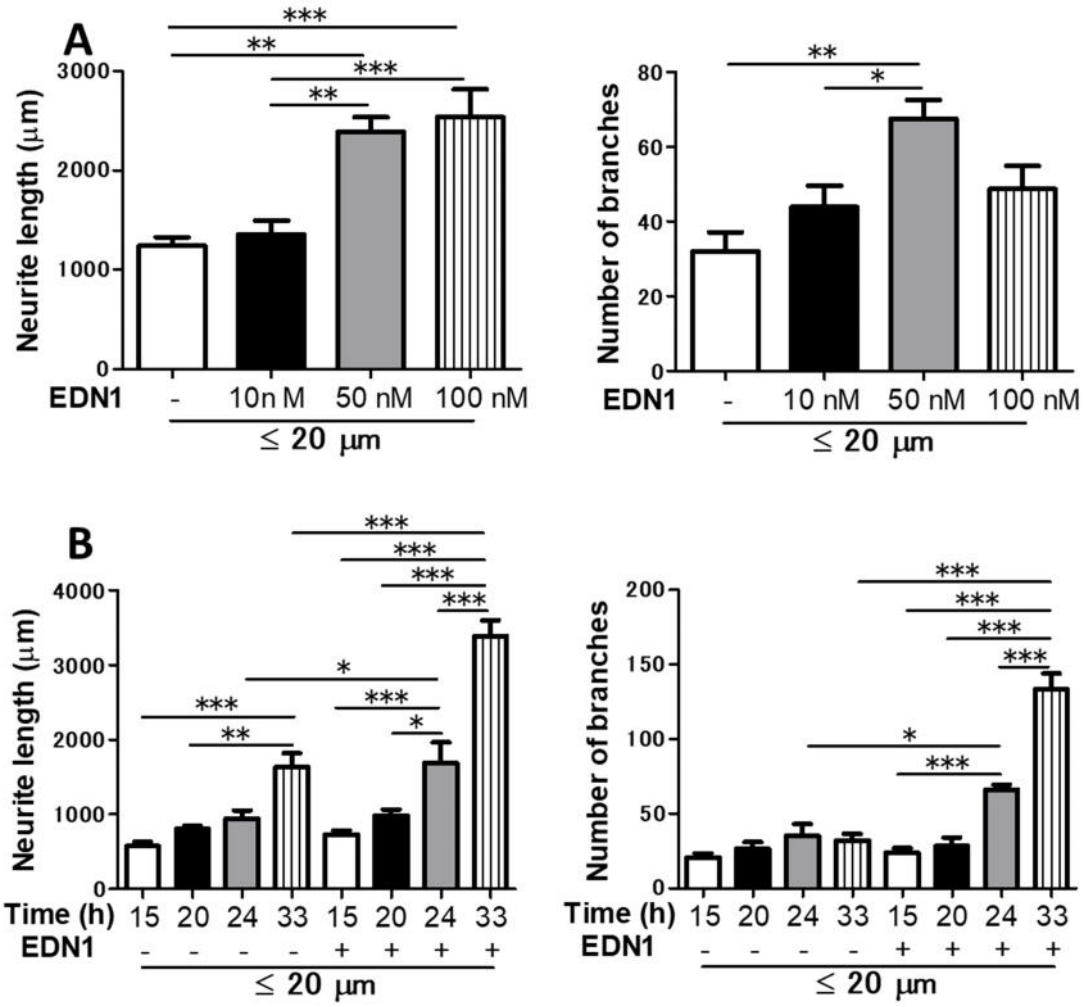

Supplementary Fig. S4. The effect of MAPK inhibitors on neurite elongation and branching in small-diameter DRG neurons. After pretreatment with or without U0126, SP600125, and SB203580, cells are stimulated with EDN1 for 24 h. Data are shown as the mean ± SEM. *p<0.05, **p<0.01, ***p<0.001.

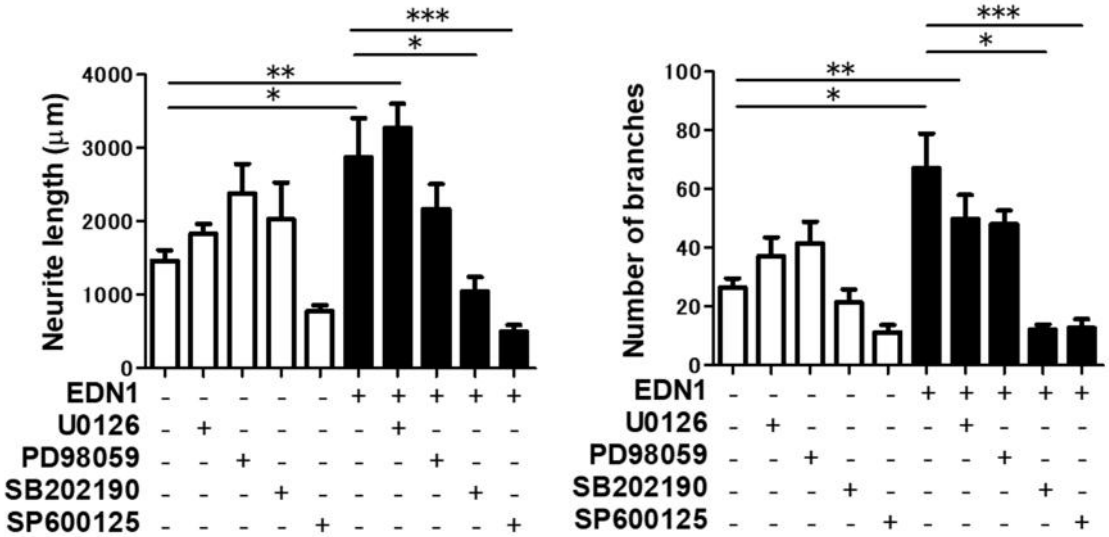

Methods

Reagents

Bosentan, an antagonist of both EDNR type A and type B, was purchased from ChemScene (Monmouth Junction, NJ). The following antibodies for immunohistochemistry and immunofluorescence staining were used: anti-eosinophil cationic protein rabbit polyclonal antibody (Proteintech, Rosemont, IL), anti-mast cell tryptase mouse monoclonal antibody (Abcam, Cambridge, UK), anti-EDN1 mouse monoclonal antibody (Abcam), anti-IL-25 mouse monoclonal antibody (Abcam), anti-protein gene product 9.5 (PGP 9.5) mouse monoclonal antibody (Abcam), anti-β3 -tubulin mouse monoclonal antibody (Sigma Aldrich, St. Louis, MO), and goat anti-mouse IgG (H+L) cross-adsorbed secondary antibody, Alexa Fluor 488 (Invitrogen, Tokyo, Japan). Mouse EDN1 was obtained from Cloud-Clone Corp. (Katy, TX). Mouse IL-31 was purchased from Peprotech (London, UK). Signal transduction inhibitors, including extracellular signal-regulated kinase (ERK)1/2 inhibitor U0126, p38 MAPK inhibitor SB203580, mitogen-activated protein kinase (MEK)1/2 inhibitor PD98059, and c-Jun N-terminal kinase (JNK) inhibitor SP600125 were purchased from Tocris (Bristol, UK).

Mice

Female NC/Nga mice aged 9–11 weeks old for the experiments on the AD-like murine

model were purchased from Charles River Laboratories Japan (Yokohama, Japan). Female C57BL/6 mice aged 6 weeks old for the experiment on DRG neuron elongation in vitro were purchased from Kyudo Co., Ltd. (Tosu, Japan). They were maintained under a 12-h light/dark cycle under specific pathogen-free conditions. This maintenance and the experimental procedures for the mice were approved by the Animal Care and Use Committee of Kyushu University School of Medicine.

Induction of mite-induced AD-like murine model

It is known that repeated epicutaneous application of mite antigen induces AD-like dermatitis in NC/Nga mice.[32] In this study, mice were anesthetized with sevoflurane and the hair on their upper back was shaved with a clipper and removed with depilatory. The shaved dorsal back and ear skin was treated with 200 mL of 4% sodium dodecyl sulfate (SDS). These mice were topically treated with 200 ml of 5% bosentan (AD-bosentan group, n=7) or vehicle (AD-ethanol group, n=7; and control-ethanol group, n=7) every day for 3 weeks on the same dorsal back and ear skin. After 1 or 2 h, 100 mg of mite antigen (*Dermatophagoides farinae* extract; Biostir AD) (Biostir Inc., Osaka, Japan) was epicutaneously applied to the same site where SDS and bosentan had been applied, twice a week for 3 weeks (AD-ethanol group and AD-bosentan group). On day 22, these mice were sacrificed (Fig. 1A).

Evaluation of skin lesions

The clinical severity of dermatitis was evaluated at every timepoint of mite antigen application. The development of 1) erythema/hemorrhage, 2) scaling/dryness, 3) edema, and 4) excoriation/erosion was scored as 0 (none), 1 (mild), 2 (moderate), or 3 (severe). The sum of the individual scores was taken as the dermatitis score.

Measurement of ear thickness in mice

The ear thickness was measured with a calibrated digital thickness gauge (Mitutoyo, Tokyo, Japan) before swabbing reagents and the difference in thickness was calculated.

Evaluation of scratching behavior

Before measurement, a small Teflon-coated columnar magnet (Ø1 mm×3 mm) was implanted subcutaneously into the back of both hind legs of the mice under sevoflurane anesthesia. The mice were placed into small observation chambers with round coils for at least 2 h for acclimation. Scratching behavior of the mice was measured for 4 h immediately after the last stimulation of mite antigen using the Microact1 system (Neuroscience Inc., Tokyo, Japan). The electric current induced by the movement of the magnet-implanted hind legs was recorded and

automatically evaluated using Microact1 software ver. 1.0.

Histological examination

Back skin tissues of mice were fixed in 10% phosphate-buffered formalin solution and then dehydrated using a Sakura autotechnicon device. After dehydration, the tissues were embedded in paraffin and cut into sections of a thickness of 3 or 5 μm (for only PGP9.5 immunohistochemistry) with a microtome (Leica Biosystems, Buffalo Grove, IL); then, they were deparaffinized and rehydrated. Sections were stained with hematoxylin/eosin. For immunohistological staining, antigens were retrieved by pressure-cooking in Histofine Heat Processor Solution (Nichirei Biosciences, Tokyo, Japan) at pH 6.0 for anti-PGP9.5 and tryptase antibody or at pH 9.0 for anti-EDN1, ECP, and IL-25 antibody for 40 min. After incubating with anti-PGP9.5 or anti-EDN1 antibody overnight at 4 , or with anti-ECP, tryptase, and IL-25 antibody for 1 h at room temperature, the sections were incubated with Histofine Simple Stain (Nichirei Biosciences), visualized with diaminobenzidine staining, and counterstained with hematoxylin. To assess the numbers of dermal inflammatory cells, eosinophils, and mast cells, five high-power fields per skin section were randomly selected from each mouse and mean cell numbers per mm^2 were counted. For the quantification of intraepidermal nerve fibers, five random photographs were taken per specimen and the number of intradermal PGP9.5-positive

nerves was counted and calculated per high-power field.

Quantitative real-time polymerase chain reaction (qRT-PCR)

Total RNA from cultured DRG neurons or ear skin of NC/Nga mice was extracted using the RNeasy Mini Kit (Qiagen, Hilden, Germany) or TRIzol reagent (Ambion, Waltham, MA), respectively, in accordance with the manufacturer's instructions. To avoid DNA contamination, total RNA was treated with DNase (Qiagen). RNA was reverse-transcribed with PrimeScript™ RT-reagent (Takara Bio Inc., Kusatsu, Japan). Subsequent qRT-PCR was carried out using SYBR Premix Ex TaqTM (TaKaRa Bio Inc.) and the CFX Connect system (Bio-Rad Laboratories, Inc., Tokyo, Japan) with the following schedule: initial denaturation and polymerase activation at 95 for 30 s, and then 40 cycles at 95 for 5 s and annealing at 60 for 30 s for *Il17* and *Ifng*, at 62 for 30 s for *Il4*, or at 66 for 30 s for *Il13*. Mouse *Tbp* was used for normalization. Fold changes of the gene expression relative to that in the control group were analyzed by the $2^{-\Delta\Delta Ct}$ method.

The primer sequences used were as follows: forward primer for mouse *Il4*, 5′-GGTCTCAACCCCCAGCTAGT-3′; reverse primer for mouse *Il4*, 5′-TGGTGTTCTTCGTTGCTGTGA-3′; forward primer for mouse *Il13*, 5′-TGAGGAGCTGAGCAACATCA-3′; reverse primer for mouse *Il13*,

5′-ATTTTGGTATCGGGGAGGCT-3′; forward primer for mouse *Il17*,

5′-GGAGAGCTTCATCTGTGTCTCTG-3′; reverse primer for mouse *Il17*,

5′-TTGGCCTCAGTGTTTGGACA-3′; forward primer for mouse *Ifng*,

5′-CGGCACAGTCATTGAAAGCCTA-3′; reverse primer for mouse *Ifng*,

5′-GTTGCTGATGGCCTGATTGTC-3′; forward primer for mouse *Tbp*,

5′-ACTCCTATGACCCCTATCACTCCTG-3′; and reverse primer for mouse *Tbp*,

5′-GTTTACAGCCAAGATTCACGGTG-3′.

ELISA

Serum obtained from the whole blood of NC/Nga mice was kept at −80 until further use. Quantikine ELISA Kit (R&D Systems, Minneapolis, MN), eotaxin mouse SimpleStep ELISA Kit (Abcam), and mouse Anti-HDM IgG Antibody Assay Kit (Chondrex, Inc., Redmond, WA) were used for detecting thymus and activation-regulated chemokine (TARC), eotaxin, and house dust mite IgG concentrations, respectively, in mouse serum, in accordance with the manufacturer's protocol.

Primary DRG neuron culture

C57BL/6 mice were deeply anesthetized by the i.p. injection of 10-fold-diluted somnopentyl.

DRGs were dissociated from the lumbar, thoracic, and cervical regions after removing blood, and then treated with papain–cysteine solution containing 0.67 mg/mL L-cysteine (Sigma Aldrich), 2 mg/mL papain (Nacalai, Kyoto, Japan), and 0.2% (v/v) saturated $NaHCO_3$ in HBSS (Nacalai) without Ca^{2+} or Mg^{2+}, and collagenase solution containing 3 mg/mL collagenase (Worthington Biochemical Corporation, Lakewood, NJ) in HBSS without Ca^{2+} or Mg^{2+}, for 10 min each at 37 . DRGs were triturated for dissociation to prepare a single-cell suspension in plating medium containing 10% FBS (Gibco, Waltham, MA), 10% horse serum (Sigma Aldrich), 1.5 mg/mL glucose, 1% penicillin/streptomycin/glutamine (Thermo Fisher Scientific, Waltham, MA), 2% B27 (Gibco), 140 µg/mL DNase (Wako, Osaka, Japan), and 2 mM GlutaMax (Gibco) in DMEM (Sigma Aldrich), followed by straining through a 70 µm cell strainer. DRG neurons were plated on poly-L-lysine-coated cover glasses (Cosmo Bio., Tokyo, Japan) coated with 0.5% laminin (Sigma Aldrich), and incubated for 4 h at 37 and 5% CO_2. Stimulation reagents were applied in feeding medium containing 1% penicillin/streptomycin/glutamine, 2% B27, and 0.5 mM GlutaMax in Neurobasal™-A medium (Thermo Fisher Scientific). Cultured DEGs were stimulated with 10, 50, or 100 nM EDN1, 6.3 nM IL-31, or medium as vehicle control for the indicated time points. In selected experiments, 100 µM bosentan, or 10 µM U0126, PD98059, SB202190, SP600125, or medium as vehicle control was applied 1 h before EDN1 stimulation.

Immunofluorescence and image analysis

Primary cultured DRG neurons were fixed in 4% paraformaldehyde (Nacalai) at room temperature for 10 min, and permeabilized with 0.2% Triton X-100 (Nacalai) in phosphate-buffered saline for 10 min. Then, they were blocked with 1% bovine serum albumin (Roche, Basel, Switzerland) and 0.1% Tween 20 (Sigma Aldrich) in phosphate-buffered saline for 30 min. Samples were incubated overnight with anti-β -tubulin antibody in blocking solution, and goat anti-mouse IgG (H+L) cross-adsorbed secondary antibody, Alexa Fluor 488, was added for 1 h. Finally, the cells were mounted with Mounting Medium with DAPI (Vector Laboratories, Burlingame, CA). Cells were observed by confocal microscopy (TCS SP8; Leica, Tokyo, Japan). The total length of all branched structures of dendrites was measured by ImageJ 1.51k (National Institutes of Health, Bethesda, MD).

Statistics

All data are presented as mean ± standard error of the mean (SEM). The statistical significance of the differences between values was determined by one-way analysis of variance, followed by Bonferroni's multiple comparison test, using GraphPad PRISM5 software Version 5.02 (GraphPad Software, La Jolla, CA). A p-value of less than 0.05 was considered statistically significant.